Phosphorus promoted trimetallic NiMoW/γ-Al$_2$O$_3$ sulfide catalysts in gas oil hydrotreating

S. Sigurdson[a], V. Sundaramurthy[a], A.K. Dalai[a,*], J. Adjaye[b]

[a] Catalysis and Chemical Reaction Engineering Laboratories, Department of Chemical Engineering, University of Saskatchewan, 57 Campus Drive, Saskatoon, SK S7N 5A9, Canada
[b] Syncrude Edmonton Research Centre, Edmonton, AB T6N 1H4, Canada

ARTICLE INFO

ABSTRACT

A series of phosphorus promoted γ-Al$_2$O$_3$-supported NiMoW sulfide catalysts consisting of 6 wt.% Mo, 7 wt.% W, 2.5 wt.% Ni and 0–2.5 wt.% P was synthesized by a co-impregnation method. The catalysts were characterized by N$_2$ adsorption, carbon monoxide chemisorption, X-ray diffraction, Raman spectroscopy, diffuse reflectance infrared Fourier transform (DRIFT) spectroscopy, X-ray absorption near edge structure (XANES) and DRIFT spectroscopy of adsorbed CO. The CO uptake measurement and Raman spectroscopy showed that P addition to NiMoW improves the dispersion of Mo and W species on the γ-Al$_2$O$_3$ surface. DRIFT spectra of adsorbed CO evidenced that the number of active sites on the surface of NiMoW/γ-Al$_2$O$_3$ sulfide increases with increasing phosphorus concentration and reaches an optimum at 1.6 wt.% of phosphorus. DRIFT spectroscopy evidenced the aluminum phosphates on the surface and also new Brønsted acid groups in P-doped catalysts. XANES study revealed that P doping in γ-Al$_2$O$_3$ does not affect the bulk electronic structure of γ-Al$_2$O$_3$. The HDS and HDN of coker light gas oil derived from Athabasca bitumen in a trickle bed reactor at industrial conditions showed that phosphorus doping has a stronger promotional effect for HDN than the HDS. The enhancement in HDN activity with phosphorus addition could be attributed more to the effect of acidity than to the improvement in dispersion. The PNiMoW/γ-Al$_2$O$_3$ catalyst with P loading of 1.6 wt.% showed superior hydrotreating activity than the bimetallic PNiMo/γ-Al$_2$O$_3$, PNiW/γ-Al$_2$O$_3$ and commercial catalysts.

© 2008 Elsevier B.V. All rights reserved.

1. Introduction

Athabasca bitumen consists of hydrocarbons in their most complex form that are mined and extracted from the Athabasca oil sands. After undergoing a fluid coking process, the crude feed is converted into light gas oil (LGO) product as well as heavy gas oil, kerosene, and naptha product streams. The LGO can be further refined to produce varying grades of gasoline and diesel fuels. However, the presence of organic sulfur and nitrogen compounds within the LGO creates problems for the final products to meet stringent emission specifications. In addition, there is also the problem of sulfur and nitrogen compounds within the LGO deactivating the noble metal catalysts applied in downstream refining processes.

Hydrotreating is the catalytic process where refined petroleum products such as LGO are reacted with hydrogen at a high temperature and pressure to remove sulfur (hydrodesulfurization, HDS) and nitrogen (hydrodenitrogenation, HDN) in the form of H$_2$S and NH$_3$ gas, respectively. A bimetallic catalyst is typically used with a metal

acting as a catalyst promoter, often cobalt or nickel, and another metal, often tungsten or molybdenum, presenting the active sites necessary for catalytic conversion. Sulfide is typically used as the active phase for the metal catalyst by forming MoS$_2$/WS$_2$ crystal structures, although nitride and phosphide active phases have been implemented as well. γ-Al$_2$O$_3$ is often used to increase the surface area and exposure sites of the metallic catalyst, although unsupported catalysts have proven to be effective in some cases.

More recently, the potential of applying trimetallic NiMoW catalysts for hydrotreatment has been explored. Nava et al. [1] and Absi-Halabi et al. [2] have reported NiMoW/γ-Al$_2$O$_3$ sulfide catalysts having higher HDS activity when compared to NiMo/γ-Al$_2$O$_3$ and NiW/γ-Al$_2$O$_3$ sulfide catalysts. A study performed by Soled et al. [3] led to the patenting of an unsupported NiMoW catalyst named NEBULA, which was found to have far greater HDS activity than supported bimetallic catalysts.

Phosphorus is currently being used as additive to improve the activity of hydrotreating catalysts. The results of studies analyzing the effect of phosphorus addition have been controversial as to whether phosphorus is promotional or detrimental to HDS and HDN activities of NiMo/γ-Al$_2$O$_3$ sulfide catalyst. While some studies have found that phosphorus promotes both HDS [4–6] and

* Corresponding author. Tel.: +1 306 966 4771; fax: +1 306 966 4777.
E-mail address: ajay.dalai@usask.ca (A.K. Dalai).

HDN [7–11] of NiMo/γ-Al$_2$O$_3$ sulfide catalyst, few reports showed no detectable effects to HDS activity from phosphorus addition [12,13]. A study performed by Nava et al. [14] found phosphorus doping to be detrimental to the activity of unsupported trimetallic NiMoW catalyst. No documented analysis was found for the effect of phosphorus on the HDS and HDN activities of supported NiMoW catalyst, specifically for a γ-Al$_2$O$_3$ support. In addition, no study has been performed for hydrotreating a real feedstock with either NiMoW/γ-Al$_2$O$_3$ sulfide catalyst or phosphorus-doped NiMoW/γ-Al$_2$O$_3$ sulfide catalyst. In this study, a series of P-doped NiMoW/γ-Al$_2$O$_3$ sulfide catalysts was prepared by the wet co-impregnation method and characterized extensively. The effect of phosphorus concentration on HDN and HDS activities of NiMoW/γ-Al$_2$O$_3$ sulfide catalyst was studied using coker light gas oil derived from Athabasca bitumen as the feed.

2. Experimental

2.1. Catalyst preparation

P-doped γ-Al$_2$O$_3$-supported NiMoW oxide catalysts were prepared by an incipient wetness co-impregnation method. The support, extruded γ-Al$_2$O$_3$ of 1 mm diameter and 8 mm length (Süd-Chemie, India) was calcined at 500 °C (ramp rate of 3 °C/min) for 3 h prior to impregnation. A series of P-doped NiO·MoO$_3$·WO$_3$/γ-Al$_2$O$_3$ precursors (6 wt.% Mo, 7 wt.% W and 2.5 wt.% Ni) with incremented amounts of P (0–2.5 wt.%) were prepared by impregnation of γ-Al$_2$O$_3$ with aqueous solution (pH ∼ 4) containing the appropriate amounts of ammonium heptamolybdate (99.9%, Aldrich), ammonium tungstate (99.9%, Aldrich), nickel nitrate (99%, BDH) and phosphoric acid (AnalaR, BDH). P-doped γ-Al$_2$O$_3$ samples were prepared by impregnation of γ-Al$_2$O$_3$ with aqueous solution containing the appropriate amounts of phosphoric acid (AnalaR, BDH). The impregnated wet samples were dried at 120 °C for 5 h and then calcined at 500 °C for 5 h in air.

2.2. Characterization techniques

The contents of Ni, Mo, W and P in the oxide form of samples were determined by inductively coupled plasma atomic emission spectroscopy (ICP-AES). Surface area, pore diameter and pore volume of oxide and sulfide forms of samples were measured by means of the adsorption of N$_2$ at 78 K using the Micromeritics ASAP 2000 instrument. The 200 mg of oxide form of sample was sulfided ex situ with 10% H$_2$S/H$_2$ at 375 °C for 4 h, and transferred to sample holder in an Ar filled glow box. Prior to the N$_2$ adsorption, each sample was degassed in vacuum at 200 °C until the static pressure remained less than 6.6 × 10^{-4} Pa. Specific surface area was determined by the Brunauer–Emmett–Teller (BET) method. Powder X-ray diffraction (XRD) patterns of the oxide and sulfide forms of samples were recorded on a Bruker diffractometer using Cu Kα radiation. Raman spectra of samples in oxide phase were recorded on a Renishaw Raman microscope (Spectra-Physics model 127) equipped with a He/Ne laser. The carbon monoxide (CO) uptake on sulfided catalysts was measured using the Micromeritics ASAP 2000 instrument. Before the chemisorption measurement, a 200 mg sample was sulfided in situ with 10% H$_2$S/H$_2$ at 375 °C for 4 h, and then evacuated until the static pressure remained less than 6.6 × 10^{-4} Pa. Pulses of CO were passed over the sample to measure the total gas uptake at 35 °C.

Diffuse reflectance infrared Fourier transform spectroscopy (DRIFTS) experiments were performed using a PerkinElmer Spectrum GX instrument equipped with DTGS detector and a KBr beam splitter. Approximately 30 mg of catalyst was loaded into a sample cup inside a Spectrotech diffuse reflectance in situ cell equipped

with ZnSe windows and a thermocouple mount that allowed direct measurement of the sample surface temperature. The oxide sample was in situ sulfided in a Spectrotech diffuse reflectance cell with 10% H$_2$S/H$_2$ at 375 °C for 2 h. At this temperature, the gas flow was switched to He at a flow rate of 50 cm^3/min and the temperature was decreased to 30 °C and then spectrum was recorded. For the CO adsorption, the sulfided sample was exposed to CO (99% pure) at a flow rate of 30 cm^3/min for 30 min. After adsorption, the system was subsequently purged with He at a flow rate of 50 cm^3/min for 60 min. The spectrum was then collected under He flow. The spectra for each experiment were averaged over 64 scans with a nominal 4 cm^{-1} resolution. Band intensities were corrected for slight differences in the weight of the catalyst and normalized to 30 mg.

X-ray absorption near edge structure (XANES) study was carried out in Variable Line Spacing Plane Grating Monochromator (VLS PGM) beamline at Canadian Light Source. The Canadian Light Source is a third generation light source, operating at 2.9 GeV energy with a critical energy of 7574 eV. The VLS PGM beamline employs three diffraction gratings to provide a very bright, highly monochromatic photon beam. The beam is tunable between 5.5 and 250 eV into the end station, solid-state absorption chamber. Two horizontal deflecting mirrors and one vertical focusing mirror direct the light from the 185 mm planar undulator through the entrance slit and onto the selected grating. The powder samples were pressed into a stainless steel sample holder and the spectra were recorded near the L-edge of the Al by measuring the fluorescence electron yield.

2.3. Catalytic activity

Hydrotreating experiments were performed in a trickle bed reactor under typical industrial conditions. The coker light gas oil (KLGO) derived from Athabasca bitumen was used as a feed for the hydrotreating studies. KLGO is a complex combination of hydrocarbons from the distillation of the products from a thermal cracking process (fluid coker). It consists of hydrocarbons having carbon numbers predominantly in the range of C$_{11}$ through C$_{28}$ and boiling in the range of 200–450 °C. It has specific gravity of 0.90 at 20 °C. It contains 0.24 and 2.3 wt.% of nitrogen and sulfur, respectively. The high pressure reaction set up used in this study simulates the process that takes place in industrial hydrotreaters. The system consists of liquid and gas feeding sections, a high-pressure reactor, a heater with temperature controller, a scrubber for removing ammonium sulfide from the reaction products, and a high-pressure gas–liquid separator. The length and internal diameter of the reactor are 240 and 14 mm, respectively. The details of catalyst loading into the reactor are described elsewhere [15]. The catalyst bed, approximately 10.5 cm long, was packed with 4 ml of catalyst diluted with 90 mesh silicon carbide. The sulfidation of catalyst was carried out by injecting 2.9 vol.% of butanethiol in straight run atmospheric gas oil (5 ml/h) at a pressure and temperature of 8.8 MPa and 193 °C, respectively, for 24 h. The H$_2$ flow rate was kept at a rate corresponding to H$_2$/sulfiding solution ratio of 600 ml/ml. The temperature of the reactor was increased to 343 °C and maintained for another 24 h. Following sulfidation, the catalyst was precoked (i.e. stabilized) with KLGO for 3 days at a temperature of 370 °C, a pressure of 8.8 MPa, and a liquid hourly space velocity (LHSV) of 1.5 h^{-1}. After precoking, HDN and HDS activities of catalysts were studied at 350, 360 and 370 °C using KLGO feed for 48 h at each temperature. The pressure, H$_2$/feed ratio and LHSV were maintained constant at 8.8 MPa, 600 ml/ml and 1.5 h^{-1}, respectively. The products were collected at 12 h intervals, and stripped with N$_2$ for removing the dissolved NH$_3$ and H$_2$S. The total nitrogen content of the liquid product was measured by combustion/chemiluminence technique following the ASTM D4629 method, and the total sulfur content was

Table 1
Elemental compositions and textural properties of P-doped NiMoW/γ-Al$_2$O$_3$

Sample	W (wt.%)	Mo (wt.%)	Ni (wt.%)	P (wt.%)	BET		
					Surface area (m^2/g)	Pore volume (cm^3/g)	Average pore diameter (nm)
γ-Al$_2$O$_3$	–	–	–	–	204	0.62	12.3
Cat-1	6.8	4.7	2.3	–	182 (178)[a]	0.50 (0.48)[a]	10.8 (11.1)[a]
Cat-2	6.4	5.1	2.3	0.5	163 (160)	0.45 (0.44)	11.1 (10.9)
Cat-3	6.4	4.8	2.2	1.0	161 (164)	0.44 (0.46)	11.0 (11.2)
Cat-4	7.1	5.1	2.4	1.3	158 (156)	0.42 (0.44)	10.7 (11.3)
Cat-5	6.9	5.2	2.4	1.6	151 (148)	0.40 (0.43)	11.1 (11.5)
Cat-6	6.7	5.1	2.2	2.0	158 (155)	0.41 (0.40)	10.6 (10.3)

[a] Value in the parenthesis represents for sulfided catalyst.

measured using combustion/fluorescence technique following the ASTM 5463 method. Both sulfur and nitrogen were analyzed in an Antek 9000 NS analyzer.

3. Results and discussion

3.1. Chemical composition and textural properties

Phosphorus-doped NiMoW/γ-Al$_2$O$_3$ catalysts with P loading of 0, 0.5, 1.0, 1.5, 2.0, and 2.5 wt.% were prepared and denoted as cat-1, cat-2, cat 3, cat-4, cat-5, and cat-6, respectively. Table 1 reports the Mo, W, Ni and P contents of each catalyst. The phosphorus contents obtained experimentally are quite close to those expected from the proportion of orthophosphoric acid used for preparing the catalysts. This is particularly true for the cat-2 and cat-3 catalysts. For cat-4 to cat-6 catalysts, a slightly lower P content is found. The Ni, Mo and W contents in all the samples are somewhat closer to the expected value of 2.5, 6 and 7 wt.%, respectively. N$_2$ adsorption tests were used to make a textural characterization of the catalysts, whose results (BET surface area, pore volume, and pore diameter) are listed in Table 1. The surface area and pore volume of P-doped catalysts are lower than the P free catalyst. The surface area and pore volume of NiMoW/γ-Al$_2$O$_3$ oxide catalyst decreased by 12 and 10%, respectively, on 0.5 wt.% of P loading, and there is no further decrease in surface area and pore volume on further P loading. Similar observation is noted with the sulfide form of catalysts. This decrease in surface area and pore volume is characteristic of a pore plugging phenomenon without change of the pore size. Indeed, as given in Table 1, there is no change in the average pore diameter of the catalyst upon P addition regardless of the P content.

3.2. Carbon monoxide chemisorption

The number of accessible surface metal atoms on trimetallic sulfide catalysts was found by chemisorption with carbon monoxide as a molecular probe. As shown in Fig. 1, a threefold increase in CO uptake of NiMoW sulfide catalysts is noted on 0.5 wt.% P loading. This confirms that P doping in NiMoW catalyst increases the dispersion of metals sulfide species. The CO uptake of P-doped NiMoW sulfide catalysts increases rapidly with an increase of P loading up to 1.3 wt.%, then it increases gradually. P introduction brought the change in surface hydroxyl groups of γ-Al$_2$O$_3$, as result impedes the formation of NiAl$_2$O$_4$ and increases the amount of Ni^{2+}(Oh) ions on the surface of the samples [16,17]. The enhanced dispersion of metals in P-doped catalysts can be due to an increase of Ni^{2+}(Oh) interactions with Mo and W.

3.3. Raman spectroscopy

XRD study of both oxide and sulfide forms of cat-1 to cat-6 (figure not given) did not show any peak other than γ-Al$_2$O$_3$ indicating
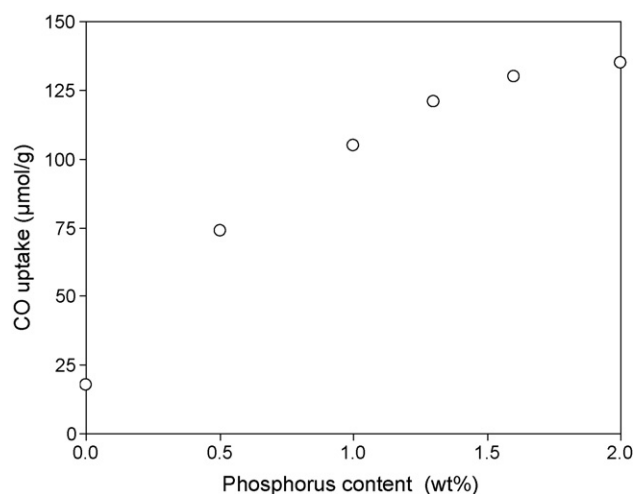

Fig. 1. Effect of phosphorus concentration on carbon monoxide uptake of sulfided NiMoW/γ-Al$_2$O$_3$ catalyst.

that the metals species are highly dispersed over the support and their particle sizes are below the detection limit of XRD technique. Raman spectra of NiMoW/γ-Al$_2$O$_3$ oxide catalysts are shown in Fig. 2. The P free sample (cat-1) shows Raman bands at 288, 663, 816 and 996 cm^{-1}. These bands correspond to MoO$_3$ crystal on the alumina surface [18]. The presence of small amounts of WO$_3$ crystal on the surface of γ-Al$_2$O$_3$ support is identified by Raman spectroscopy in cat-1. A small band at 992 cm^{-1} corresponding to WO$_3$ crystal [19] is evident in enlarged spectra. This band is not present in P-
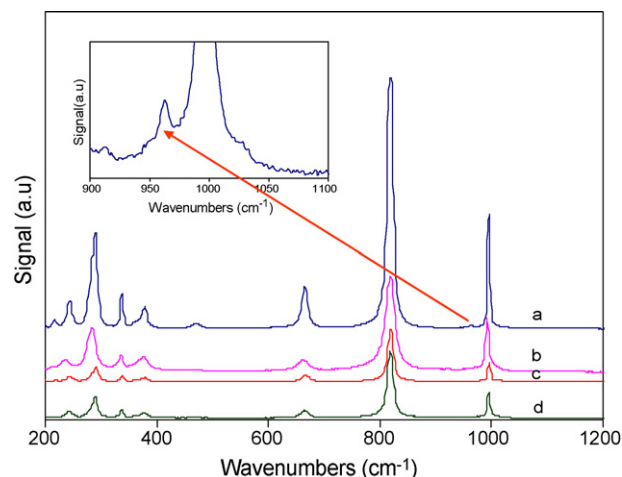

Fig. 2. Raman spectra of NiMoW/γ-Al$_2$O$_3$ oxide catalysts: (a) cat-1, (b) cat-2, (c) cat-3, and (d) cat-4.

doped catalysts. As shown in Fig. 2, the intensity of all the bands of MoO_3 crystal decreases by 50% on 0.5 wt.% P loading and decreases more on further P loading. The bands disappear completely with P loading of 1.6 wt.% and higher. At higher P loading ($\geq$1.6 wt.%), the crystal size of MoO_3 drops below the detection limit of Raman spectroscopy. The decrease of Raman band intensity is evidence that P doping increases the dispersion of MoO_3 and WO_3 crystals on γ-Al_2O_3 support. Raman spectra obtained at different points on P-doped (cat-2 to cat-4) catalysts were more consistent compared to cat-1. A greater homogeneity of the MoO_3 component was observed on the external surface of cat-4 than the cat-1. This evidences that P doping has increased the MoO_3 phase homogeneity on catalyst surface.

3.4. DRIFT spectroscopy

The time need for sulfidation of catalysts at 375 °C with 10% H_2S/H_2 was studied by DRIFT spectroscopy. A 30 mg of sample was loaded in the *in situ* cell and the sample was heated to 375 °C at a ramp rate of 3 °C/min. The DRIFT spectrum of oxide form of catalysts show main band at 1009 cm^{-1} due to terminal Mo=O groups stretching vibration and the broad bands at 820 and 880 cm^{-1} due to Mo–O vibrations of the MoO_3 lattice (figure not given). The intensity of above-mentioned bands was decreasing with time of sulfidation up to 90 min. There was no change in intensity of these bands after 90 min. This showed that sulfidation time of 90 min at 375 °C is enough to get the optimum sulfidation. Hence all the catalysts were *in situ* sulfided for 120 min at 375 °C using 10% H_2S/H_2. *In situ* DRIFT spectra of the hydroxyl region of sulfided catalysts and γ-Al_2O_3 are shown in Fig. 3. The γ-Al_2O_3 shows a shoulder band at 3765 cm^{-1}, and broad bands at 3731, 3677 and 3580 cm^{-1}. Based on literature [16] these bands can be assigned to the most basic hydroxyl, the basic hydroxyl, the most acidic hydroxyl and hydrogen-bonded water groups, respectively. The spectrum of cat-1 shows that an impregnation of NiMoW metals on γ-Al_2O_3 results
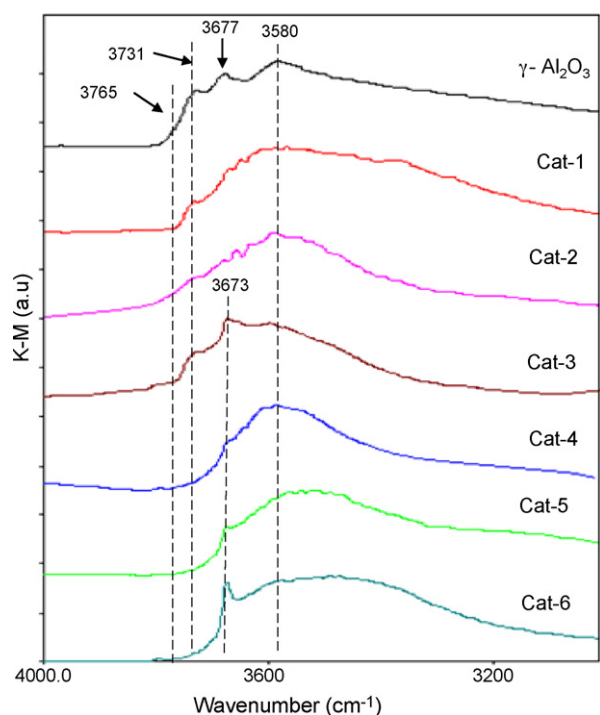
disappearance of most basic and acidic hydroxyl groups and also weakens the peak at 3731 cm^{-1}. P doping of 0.5 wt.% in NiMoW/γ-Al_2O_3 catalyst further weakens the band at 3731 cm^{-1}. For the samples with P content at 1.3 wt.% and above, this band is not observed at all. A new band at 3673 cm^{-1} emerges at 1.0 wt.% P loadings and above. This band intensity is increasing with P loading and well resolved as a sharp peak at higher P loadings. These results show that phosphoric acid reacts with alumina hydroxyl groups and also creates new OH groups (Brønsted acid sites). The added Ni, Mo and W metals covered the hydroxyl groups of γ-Al_2O_3, hence it is difficult to study the interaction of P on hydroxyl groups of alumina support by DRIFT spectroscopy. To elucidate the effect of P on the hydroxyl groups of γ-Al_2O_3, a series of P modified γ-Al_2O_3 with various P loadings was prepared and studied by DRIFT spectroscopy. The P modified γ-Al_2O_3 samples also studied in the sulfide form as P-doped NiMoW/γ-Al_2O_3 catalysts. The DRIFT spectra of the hydroxyl region of sulfided P-doped γ-Al_2O_3 (with P loadings varied from 0.0 to 2.5 wt.%) are shown in Fig. 4. The weakening of the IR bands at 3765 and 3731 cm^{-1} on 0.5 wt.% of P loadings indicates that phosphoric acid initially reacts with basic alumina hydroxyl groups. Increasing the phosphorous loading to 1.5 wt.% results in the complete loss of the both basic hydroxyl bands. The intensity of the acidic alumina hydroxyl band also starts to decrease from 1.5 wt.% of P loading. This shows that phosphoric acid reacts with all the hydroxyl groups of alumina at 1.5 wt.% of P loadings. Finally, as the P loading is increased to 2.0 wt.%, a sharp band at 3673 cm^{-1}, which was observed with P-doped NiMoW catalysts, also appeared and become predominant at 2.5 wt.% of P loadings.

Phosphoric acid, which has three hydroxyl groups attached to the phosphorus atom, interacts with the surface hydroxyls of alumina by single bond or multiple bonds. The single- or multiple-bond formation depends on the availability of γ-Al_2O_3 hydroxyl
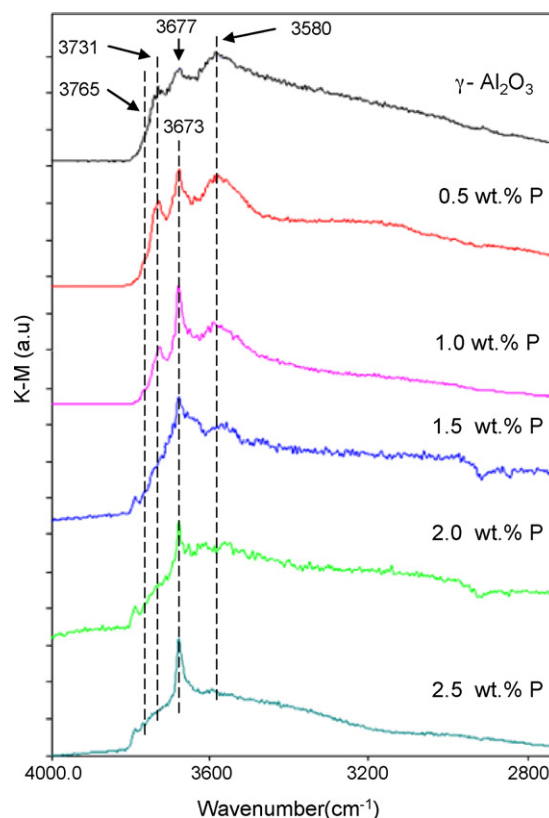

Fig. 3. DRIFT spectra of γ-Al_2O_3 and NiMoW/γ-Al_2O_3 sulfide catalysts in the OH region.

Fig. 4. DRIFT spectroscopy of γ-Al_2O_3 and P-doped γ-Al_2O_3 samples in the OH region.
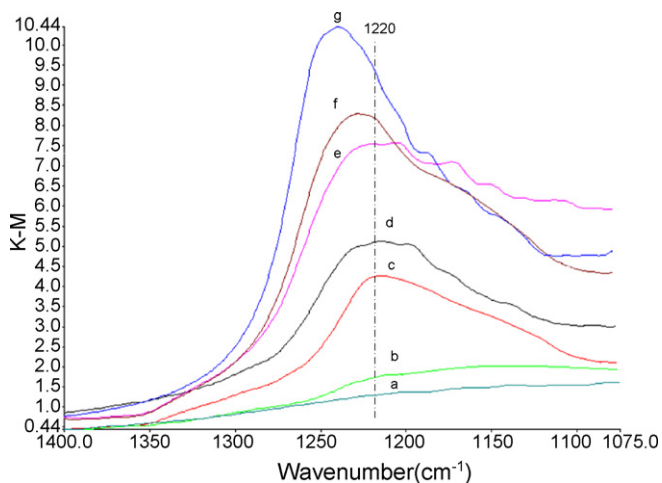
Fig. 5. DRIFT spectroscopy of γ-Al$_2$O$_3$ and NiMoW/γ-Al$_2$O$_3$ sulfide catalysts in the P–O bond region: (a) γ-Al$_2$O$_3$, (b) cat-1 (c) cat-2, (d) cat-3, (e) cat-4, (f) cat-5 and (g) cat-6.

groups and the amount of phosphoric acid. This study showed that up to 1.5 wt.% P loadings, phosphoric acid interacts with γ-Al$_2$O$_3$ by multiple bonds and hence decreases the OH band's intensity. Phosphoric acid interacts with alumina by a single bond at 2.0 wt.% P and higher loadings, therefore, the other two hydroxyl groups of the phosphoric acid (P–OH) remain unbound on the catalyst surface. In this study, the observed sharp band at 3673 cm^{-1} with P-doped γ-Al$_2$O$_3$ and NiMoW catalysts at higher P loadings can be due to the formation of P–OH group on the surface. Müller et al. [20] studied the AlPO-5 materials by infrared spectroscopy and assigned a 3675 cm^{-1} peak to the terminal P–OH group. Decanio et al. [16] also observed a similar IR peak in 4 wt.% P loaded γ-Al$_2$O$_3$ and assigned this peak to phosphate associated OH groups.

To study the nature of phosphates, DRIFT spectroscopy study was carried out in the 1400–1000 cm^{-1} region. Fig. 5 shows the *in situ* DRIFT spectra of sulfided NiMoW/γ-Al$_2$O$_3$ catalysts in the P–O bond stretching region. For all P-doped samples, a broad band is observed from 1300 to 1100 cm^{-1} with a shift to a higher wave number with an increase in the phosphorus content. The band intensity is increasing with P concentration. The position of this band corresponds to the P–O bond vibrations of [PO$_4$]$^{3-}$, [HPO$_4$]$^{2-}$ and [H$_2$PO$_4$]$^{1-}$ groups in aluminum phosphates [21]. The ^{32}P MAS-NMR study by Decanio et al. [16] showed the presence of monomeric, polymeric, amorphous and crystalline aluminum phosphates in the oxide form of P-doped alumina-supported NiMo hydrotreating catalyst. They also found that the amount of each phase was varying with the P concentration. In the present study, the P–O bond of aluminum phosphate becomes stronger upon increasing the P content and is reflected in the DRIFT spectra by a shift of the P–O band to a higher wave number. The [PO$_4$]$^{3-}$ displays the weakest P–O bond, whereas protonated phosphates such as [HPO$_4$]$^{2-}$ and [H$_2$PO$_4$]$^{1-}$ show the highest P–O bond strength [22]. The shift of the P–O band shows that a protonated phosphate ion, [H$_2$PO$_4$]$^{1-}$ is formed at higher P loading. This is akin to DRIFT study of the OH region, which is also evidence that phosphoric acid interacts with the OH groups of Al with multiple bonds at lower P concentrations, and leads to [PO$_4$]$^{3-}$ species. The single bond interaction at higher P concentrations leads to [H$_2$PO$_4$]$^{1-}$ species.

To study whether phosphate formed only on the surface or in the bulk of γ-Al$_2$O$_3$, Al L-edge XANES was studied. The XANES spectra of γ-Al$_2$O$_3$ and selected catalysts are shown in Fig. 6. The XANES spectra of γ-Al$_2$O$_3$ can be characterized at a main peak at 80 eV, a shoulder peak at 78 eV and a broad peak at 84.5 eV. From the fig-
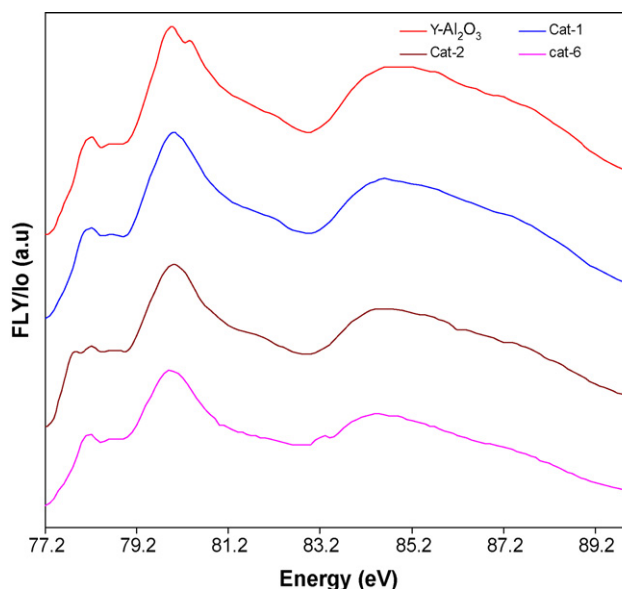

Fig. 6. Al L-edge XANES spectra of γ-Al$_2$O$_3$ catalysts and selected P-doped NiMoW/γ-Al$_2$O$_3$.

ure, it is observed that XANES peaks of P-doped γ-Al$_2$O$_3$-supported catalysts match with the γ-Al$_2$O$_3$ peaks. Fluorescence yield (FLY) monitors preferentially the bulk of the specimen at this photon energy. This indicates that the P doping does not affect the bulk electronic structure of γ-Al$_2$O$_3$. DRIFT study evidenced the aluminum phosphate species in P-doped aluminum-supported catalysts. As there is no change in the bulk electronic structure of γ-Al$_2$O$_3$ on P doping as evidenced by the XANES study, it confirms that aluminum phosphates phases are formed only on the surface of γ-Al$_2$O$_3$.

The surface active sites of the NiMoW sulfide catalysts were studied by using DRIFT spectroscopy combined with CO as a probe molecule. This study was done at 30 °C to avoid CO adsorption on γ-Al$_2$O$_3$ and to achieve CO adsorption only on metal sulfide. Fig. 7 shows the DRIFT spectra of CO adsorbed on sulfided cat-1 to cat-6. There are six overlapping bands between 2100 and 2000 cm^{-1}, apparent in all the catalysts irrespective of P concentration. No new band was observed on P doping, instead, change in band intensity was noted. The NiMoW/γ-Al$_2$O$_3$ sulfide catalyst could possess surface active sites, such as Mo–S, W–S, Ni–Mo–S, Ni–W–S and Ni–Mo–W–S phases [23]. Discrimination of these complex sur-
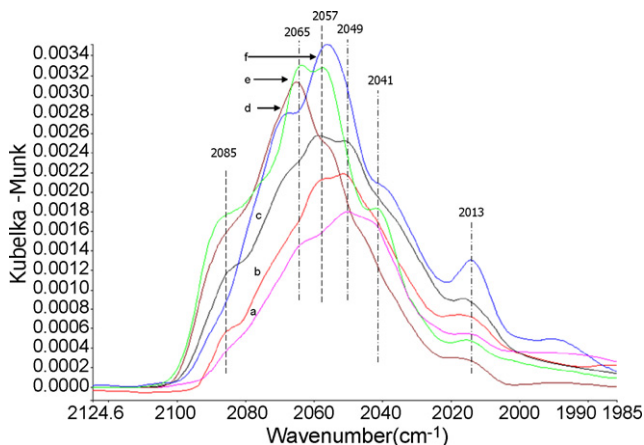

Fig. 7. DRIFT spectra of adsorbed CO on NiMoW/γ-Al$_2$O$_3$ sulfide catalysts: (a) cat-1 (b) cat-2, (c) cat-3, (d) cat-4, (e) cat-5 and (f) cat-6.

face active sites by DRIFT of CO adsorption was not possible in the present study because of band overlapping. But, the P doping effect in NiMoW/γ-Al$_2$O$_3$ is clearly visible in DRIFT spectra of adsorbed CO. The P-doped catalysts (cat-2 to cat-6) showed increased CO adsorption band intensity compared with P free NiMoW/γ-Al$_2$O$_3$ (cat-1) catalyst. This is evidence of an increase in the number of surface sites for NiMoW/γ-Al$_2$O$_3$ sulfide catalyst with P doping. All these bands are increasing with increase in P concentration and reached an optimum at 1.6 wt.% P loading. This confirms that 1.6 wt.% P loading in NiMoW/γ-Al$_2$O$_3$ is sufficient to get optimum surface active sites. The CO uptakes study also proved that 1.6 wt.% P loading is sufficient to get maximum dispersion. The surface active sites are formed by the interaction of Ni^{2+}(Oh) with Mo and W sulfides. The P introduction impedes the formation of NiAl$_2$O$_4$ (if formed, reduces activity) and increases the amount of Ni^{2+} (Oh) ions on the surface of the samples [16,17]. The increase of Ni^{2+} (Oh) ions concentration with an increase of P loadings leads to increase in the amount of the surface active sites.

3.5. Hydrotreating activity

The hydrotreating activity of catalysts was tested using coker light gas oil derived from Athabasca bitumen. To achieve steady-state activity, the sulfided catalysts were precoked for 72 h at a temperature, pressure, LHSV and H$_2$/feed ratio of 370 °C, 8.8 MPa, 1.5 h^{-1} and 600 ml/ml, respectively. The HDN and HDS activities decreased gradually by 6–9% during first 48 h because of coke deposition on the catalyst surface. The HDN and HDS activities remained constant thereafter. After precoking, the steady-state activity of all the prepared catalysts were studied using the same feed at reaction temperatures of 350, 360 and 370 °C, a pressure of 8.8 MPa, a LHSV of 1.5 h^{-1} and a hydrogen/gas oil ratio of 600 ml/ml. The activity was studied for 48 h at each temperature. The samples were collected at every 12 h. The average N and S conversion of last two samples at each reaction temperature are shown in Figs. 8 and 9, respectively. The conversion for the two samples taken at each reaction condition differed by no greater than 1.5%.

The results from Figs. 8 and 9 show an almost uniform consistency as nitrogen and sulfur conversion rise with the increase in catalyst phosphorus content from cat-1 to cat-5. However, the con-
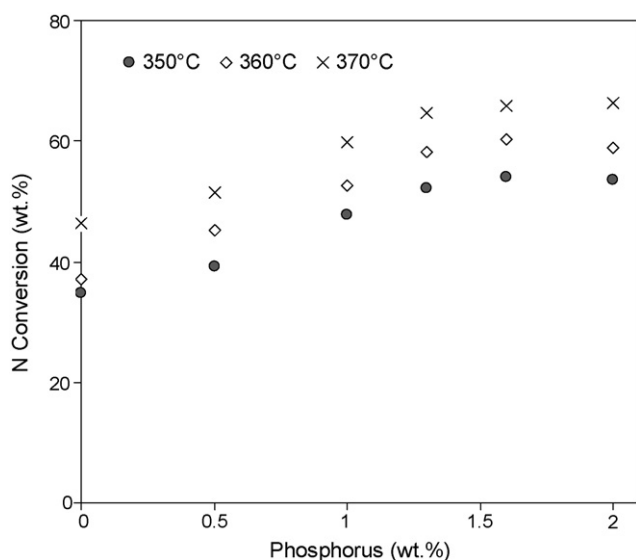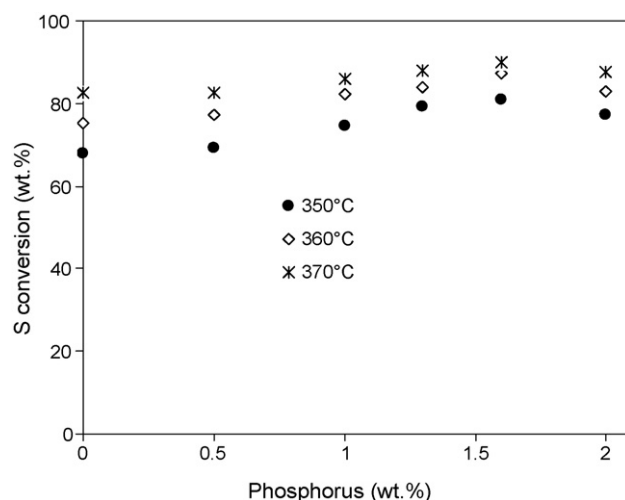

Fig. 9. Effect of P concentration in NiMoW/γ-Al$_2$O$_3$ catalyst on HDS of KLGO at different temperatures. $P = 8.8$ MPa, LHSV = 1.5 h^{-1} and H$_2$/oil = 600 (ml/ml).

versions determined for cat-6 showed that the further increase in phosphorus content produced negligible improvement in HDN and HDS activities. From these results, it was concluded that cat-5 was the optimum prepared catalyst, having an intended phosphorus content of 2.0 wt.% and an actual phosphorus content of 1.6 wt.%. Using a reaction temperature of 360 °C as a basis of comparison, cat-5 showed an HDN conversion of 60.4% compared to 37.0% for cat-1, and an HDS activity of 87.3% compared to 75.1% for cat-1. The observed effectiveness of phosphorus as a catalyst promoter for HDN and HDS activities is attributed to a greater dispersion of the metals on the catalyst surface. This increase in the dispersion of the transition metals on the γ-Al$_2$O$_3$ surface was observed during Raman spectroscopy and CO chemisorption studies of the catalysts. The clusters of metal sulfides that would normally form on the catalyst surface in the absence of phosphorus can result in restricted access to active sites. By increasing the coverage of the transition metals on the catalyst surface, the number of metal sulfide active sites that become accessible for feed molecules increases. It can also be observed from the HDN and HDS activities that the increase in phosphorus content of the catalyst had a greater effect on the conversion of nitrogen than it did for sulfur. For example at 360 °C, the HDN conversion increased by 57%, while HDS conversion increased only by 12% for 1.6 wt.% of P addition. This reveals that the explanation about the influence of P on HDN activity of NiMoW/γ-Al$_2$O$_3$ sulfide catalyst would not reside only in the increase of dispersion and number of surface active sites, but also in the mechanism and the rate determining step of HDS and HDN reactions.

Both the HDN and HDS reaction networks have two main steps, hydrogenation (HYD) and hydrogenolysis (C–S or C–N bond breaking), that take place on different sites [24,25]. Hydrogenolysis takes place on Brønsted acid sites originating from H$_2$S adsorption on the metal sulfide or from the phosphate promoter. Hydrogenation occurs on metal sulfide species, with sulfur vacancies [25]. The C–N bond breaking is the slowest step in the HDN reaction network. P addition created the new Brønsted acid sites as evidenced by DRIFT study. The newly formed Brønsted acid sites can increase the C–N bond breaking (rate limiting step) and thus enhances HDN activity. The less significant increase in HDS activity from the addition of phosphorus can be explained by the C–S bond found in organic sulfur compounds being much weaker than C–N bonds, therefore C–S bond breaking is not limiting the rate of HDS reaction. For HDS, hydrogenation, the slower of the two steps, occurs on the metal sulfide species, which have sulfur vacancies [25].
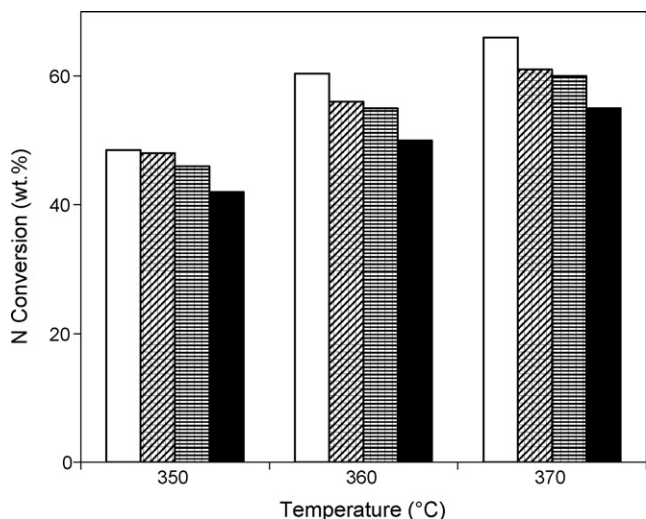

Fig. 8. Effect of P concentration in NiMoW/γ-Al$_2$O$_3$ catalyst on HDN of KLGO at different temperatures. $P = 8.8$ MPa, LHSV = 1.5 h^{-1} and H$_2$/oil = 600 (ml/ml).

Fig. 10. Comparison of HDN activity of optimum NiMoW/γ-Al$_2$O$_3$ catalyst with commercial and bimetallic sulfide catalysts at different temperatures. (□) cat-5, (▨) commercial, (▤) NiMo, (■) NiW, P = 8.8 MPa, LHSV = 1.5 h^{-1} and H$_2$/oil = 600 (ml/ml).

Fig. 11. Comparison of HDS activity of optimum NiMoW/γ-Al$_2$O$_3$ catalyst with commercial and bimetallic sulfide catalysts at different temperatures. (□) cat-5, (▨) commercial, (▤) NiMo, (■) NiW, P = 8.8 MPa, LHSV = 1.5 h^{-1} and H$_2$/oil = 600 (ml/ml).

The effect of acidity created by P for HDS of these samples depends possibly on whether the rupture of C–S or C–N bonds is slower or faster than hydrogenation. The hydrogenolysis and hydrogenation routes in HDS reaction depend on the nature of compound, the catalyst (CoMo or NiMo), the H$_2$S partial pressure, and the total pressure. NiMo/Al$_2$O$_3$ (generally regarded as superior to CoMo/Al$_2$O$_3$) as a hydrogenation catalyst favors the HYD route compared with CoMo/Al$_2$O$_3$ catalyst. Hydrogenolysis is the preferred route in HDS of simple compounds like thiophene and benzothiophene, but the substituted benzothiophenes favor the hydrogenation route [26,27]. P addition to CoMo/γ-Al$_2$O$_3$ favors the HYD route in HDS of dibenzothiophene [16]. The study by Rabarihoela-Rakotovao et al. [28] showed that hydrogenolysis route of dibenzothiophenes is inhibited by the H$_2$S partial pressure and thus favors HYD route. Further, an increase in total pressure from 2.5 to 5.5 MPa increased the rate ratio of HYD to hydrogenolysis from 0.6 to 1 [28]. In the present study, the HDN and HDS of KLGO were carried at 8.8 MPa over P-doped NiMoW/γ-Al$_2$O$_3$ sulfide catalysts. The above reaction pressure and catalyst type can favor the HYD route in HDS of KLGO. It may also be noted that KLGO contains mostly substituted benzothiophenes, which can also favor the HYD route. Further, the higher amount of S (2.3 wt.%) in the feed and more than 50 wt.% conversion of sulfur leads to a higher H$_2$S partial pressure and thus lead HYD route in HDS of KLGO.

The best trimetallic PNiMoW/γ-Al$_2$O$_3$ catalyst (cat-5) was compared with the P-doped bimetallic catalysts, PNiMo/γ-Al$_2$O$_3$ (13 wt.% Mo, 2.4 wt.% Ni and 1.7 wt.% P) and PNiW/γ-Al$_2$O$_3$ (13 wt.% Wo, 2.4 wt.% Ni and 1.6 wt.% P) of similar metals loadings. The hydrotreating activity of these catalysts was compared at reaction temperatures of 350, 360 and 370 °C, a pressure of 8.8 MPa, a LHSV of 1.5 h^{-1} and a hydrogen/gas oil ratio of 600 ml/ml. The results are shown in Figs. 10 and 11. The trimetallic catalyst shows higher hydrotreating activity at all three temperatures among the catalysts. For example, at 360 °C, the N and S conversion of trimetallic catalyst are higher than the bimetallic NiMo catalyst by 9 and 13%, respectively. Similarly, 15 and 21% increases in N and S conversion, respectively, were observed over trimetallic catalyst when compared with bimetallic NiW catalyst. The above results are evidence of the superiority of the trimetallic catalyst over the bimetallic catalysts.
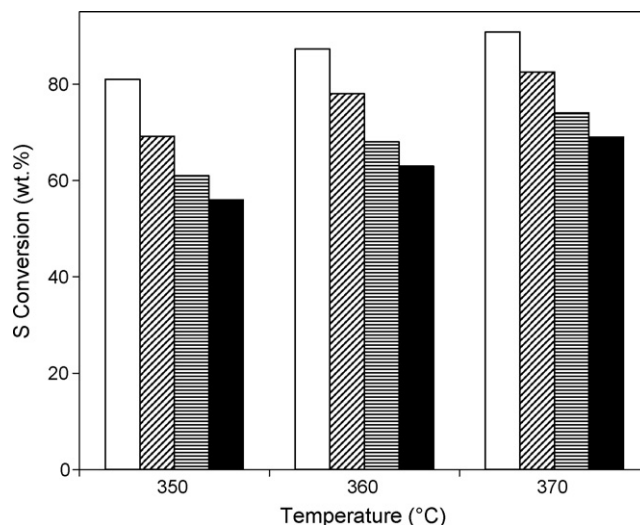
To determine how effective the optimum cat-5 catalyst would be if applied for industrial applications, the results of its HDN & HDS activities were compared to those obtained from implementing a commercial P-doped bimetallic NiMo sulfide catalyst (Criterion) in the same experimental apparatus, procedure, and conditions. The results for the nitrogen and sulfur conversion of the commercial catalyst were determined by the same method as they were for the self-prepared catalysts and shown in Figs. 10 and 11, respectively. It can be seen from these results that cat-5 consistently showed superior HDN and HDS activities for each reaction temperature. Using 360 °C once again as a basis of comparison, the self-prepared cat-5 converted 60.4% of nitrogen present in the KLGO compared to 56.0% for the commercial catalyst. In addition, cat-5 converted 87.3% of KLGO sulfur content compared to 78.0% for the commercial catalyst.

4. Conclusions

The catalytic activity for HDN increases substantially more compared to HDS of coker gas oil at industrial conditions when phosphorus is added to NiMoW/γ-Al$_2$O$_3$ as a promoter. From the results of the Raman spectroscopy, CO chemisorption, and DRIFT spectroscopy of adsorbed CO, it is evident that P doping improves the dispersion and number of surface active sites. These effects then give rise to the enhancement of the HDN and HDS activities of the P-doped NiMoW/γ-Al$_2$O$_3$ catalysts. When P is added to NiMoW/γ-Al$_2$O$_3$, the HDN and HDS activities steadily increase with the P content up to an optimum concentration of 1.6 wt.%. At this concentration, the P-doped trimetallic catalyst shows better hydrotreating activity than the bimetallic and commercial catalysts. It is apparent from DRIFT spectroscopy that the P doping creates new acidic sites in NiMoW/γ-Al$_2$O$_3$ catalysts. The acidic sites brought by phosphorus accelerates the C–N bond breaking, a rate determining step, and promotes the HDN activity to a higher degree than the HDS activity with coker gas oil.

cial support. The authors are also grateful to Canadian Light Source (CLS) for their support in the XANES study.

References

[1] H. Nava, F. Pedraza, G. Alonso, Catal. Lett. 99 (2005) 65.
[2] M. Absi-Halabi, A. Stanislaus, K. Al-Dolama, Fuel 77 (1998) 787.
[3] S.L. Soled, S. Miseo, R. Krikak, H. Vroman, T.H. Ho, K.L. Riley, US Patent 6,299,760 B1 (2001).
[4] S. Eijsbouts, J.N.M. van Gestel, J.A.R. van Veen, V.H.J. de Beer, R. Prins, J. Catal. 131 (1991) 412.
[5] J.A.R. van Veen, H.A. Colijn, P. Hendriks, A.J. van Welsenes, Fuel Process. Technol. 35 (1993) 137.
[6] C. Liu, Y. Yu, H. Zhao, Fuel Process. Technol. 86 (2004) 449.
[7] Y.W. Chen, W.C. Hsu, C.S. Lin, B.C. Kang, S.T. Wu, L.J. Leu, J.C. Wu, Ind. Eng. Chem. Res. 29 (1990) 1830.
[8] J.M. Lewis, R.A. Kydd, J. Catal. 136 (1992) 478.
[9] R.A. Kemp, C.T. Adams, Appl. Catal. A 134 (1996) 299.
[10] Y. Park, E. Oh, H. Rhee, Ind. Eng. Chem. Res. 38 (1997) 5083.
[11] P. Atanasova, T. Halachev, J. Uchytil, M. Kraus, Appl. Catal. A 38 (1998) 235.
[12] J. Fierro, A. Lopez-Agudo, N. Esquivel, R. Lopez-Cordero, Appl. Catal. A 48 (1989) 353.
[13] S.M.A.M. Bouwens, J.P.R. Vissers, V.H.J. De Beer, R. Prins, J. Catal. 112 (1988) 401.
[14] H. Nava, J. Espino, G. Berhault, G. Alonso-Nunez, Appl. Catal. 302 (2006) 177.
[15] V. Sundaramurthy, A.K. Dalai, J. Adjaye, Catal. Lett. 102 (2005) 299.
[16] E.C. DeCanio, J.C. Edwards, T.R. Scalzo, D.A. Storm, J.W. Bruno, J. Catal. 132 (1991) 498.
[17] P. Atanasova, T. Tabakova, Ch. Vladov, T. Halachev, A.L. Agudo, Appl. Catal. A 161 (1997) 105.
[18] G. Lebourdon, F. Adar, M. Moreau, S. Morel, J. Reffner, A.S. Mamede, C. Dujardin, E. Payen, Phys. Chem. Chem. Phys. 5 (2003) 4441.
[19] K. Nonaka, A. Takase, K. Miyakawa, J. Mater. Sci. Lett. 12 (1993) 274.
[20] G. Müller, J. Bódis, J. Kornatowski, Microporous Mesoporous Mater. 69 (2004) 1.
[21] M. Rokita, M. Handke, W. Mozgawa, J. Mol. Catal. 450 (1998) 213.
[22] P.N. Persson, N. Isson, S. Sjoberg, J. Colloid Interface Sci. 177 (1996) 263.
[23] C. Thomazeau, C. Geantet, M. Lacroix, M. Danot, V. Harlé, P. Raybaud, Appl. Catal. A 322 (2007) 92.
[24] V. Vanrysselberghe, G.F. Froment, Ind. Eng. Chem. Res. 35 (1996) 3311.
[25] S.H. Yang, C.N. Satterfield, J. Catal. 81 (1983) 168.
[26] J.M. Herrera, J. Reyes, P. Roquero, T. Klimova, Microporous Mesoporous Mater. 83 (2005) 283.
[27] R. Prins, M. Egorova, A. Rothlisberger, Y. Zhao, N. Sivasankar, P. Kukula, Catal. Today 111 (2006) 84.
[28] V. Rabarihoela-Rakotovao, S. Brunet, G. Perot, F. Diehl, Appl. Catal. A 306 (2006) 34.